Beam Hardening Correction via Mass Attenuation Discretization

Renliang Gu and Aleksandar Dogandžić {renliang, ald}@iastate.edu
Department of Electrical and Computer Engineering
IOWA STATE UNIVERSITY

Background

According to the Lambert-Beer's law [Jenkins and White 1957], the fraction $\mathrm{d}\mathcal{I}/\mathcal{I}$ of plane wave intensity lost in traversing an infinitesimal thickness $\mathrm{d}\ell$ at Cartesian coordinates (x, y) is proportional to $\mathrm{d}\ell$, so that

$$\frac{\mathrm{d}\mathcal{I}}{\mathcal{I}} = -\mu(\varepsilon)\alpha(x, y)\,\mathrm{d}\ell.$$

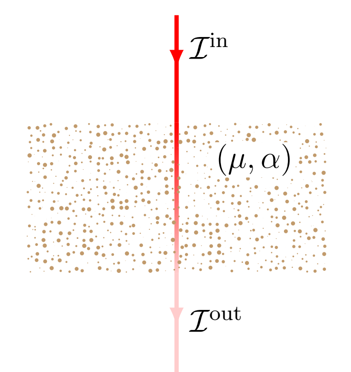

where
- $\mu(\varepsilon)$ is the *mass attenuation coefficient* of the material (in $\frac{\text{cm}^2}{\text{g}}$), which depends only on the photon energy ε,
- $\alpha(x, y)$ is the density map of the inspected object (in $\frac{\text{g}}{\text{cm}^3}$).

Therefore, a monochromatic X-ray signal at photon energy ε attenuates *exponentially* as it penetrates an object composed of a single material:

$$\mathcal{I}^{\text{out}} = \mathcal{I}^{\text{in}} \exp\Big[-\mu(\varepsilon)\int_\ell \alpha(x, y)\,\mathrm{d}\ell\Big].$$

where $\mathcal{I}^{\text{out}}$ and $\mathcal{I}^{\text{in}}$ are the emergent and incident X-ray signal energies, respectively.

However, X-rays generated by vacuum tubes are not monochromatic. To describe the polychromatic X-ray source, assume that its incident intensity $\mathcal{I}^{\text{in}}$ spreads along photon energy ε following the density $\iota(\varepsilon)$, i.e.,

$$\int \iota(\varepsilon)\,\mathrm{d}\varepsilon = \mathcal{I}^{\text{in}}. \tag{1a}$$

Then, the noiseless measurement collected by an energy integral detector upon traversing a straight line $\ell = \ell(x, y)$ is

$$\mathcal{I}^{\text{out}} = \int \iota(\varepsilon) \exp\Big[-\mu(\varepsilon)\int_\ell \alpha(x, y)\,\mathrm{d}\ell\Big]\,\mathrm{d}\varepsilon. \tag{1b}$$

Polychromatic X-ray CT Model via Mass Attenuation

Assumption:
- Both incident spectrum $\iota(\varepsilon)$ and mass attenuation function $\mu(\varepsilon)$ of the object are *unknown*.

Objective:
- Estimate the density map $\alpha(x, y)$.

Based on the fact that mass attenuation $\mu(\varepsilon)$ and incident spectrum density $\iota(\varepsilon)$ are both functions of ε (see Fig. 1), our **idea** is to:
- write the model as integrals of μ rather than ε;
- estimate $\imath(\mu)$ rather than $\iota(\varepsilon)$ and $\mu(\varepsilon)$.

For invertible $\mu(\varepsilon)$, define its inverse as $\varepsilon(\mu)$ and rewrite (1a) and (1b) as

$$\mathcal{I}^{\text{in}} = \int \imath(\mu)\,\mathrm{d}\mu, \qquad \mathcal{I}^{\text{out}} = \int \imath(\mu) \exp\Big[-\mu\int_\ell \alpha(x, y)\,\mathrm{d}\ell\Big]\,\mathrm{d}\mu \tag{2}$$

where

$$\imath(\mu) \triangleq \iota(\varepsilon(\mu))|\varepsilon'(\mu)|$$

and $\varepsilon(\mu)$ is differentiable with derivative $\varepsilon'(\mu) = \frac{\mathrm{d}\varepsilon(\mu)}{\mathrm{d}\mu}$. Invertibility of $\mu(\varepsilon)$ is assumed for simplicity: easy to extend (2) to arbitrary $\mu(\varepsilon)$.

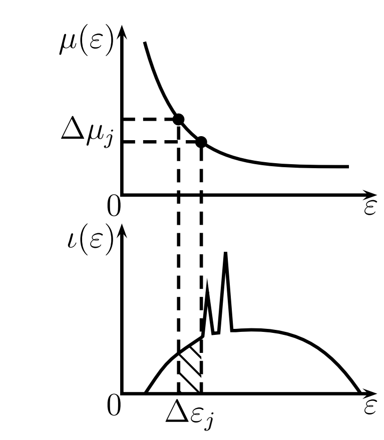

Figure 1: Mass attenuation and incident spectrum as functions of photon energy ε.

Discretizations over Mass Attenuation

Discretize (2) in the mass attenuation and spatial domains using J mass attenuation bins and p pixels:

$$\mathcal{I}^{\text{in}} = \sum_{j=1}^{J} \mathcal{I}_j \quad \text{and} \quad \mathcal{I}^{\text{out}} = \sum_{j=1}^{J} \mathcal{I}_j \mathrm{e}^{-\mu_j \boldsymbol{\phi}^T \boldsymbol{\alpha}} \tag{3}$$

where
- $\boldsymbol{\alpha}$ is a $p \times 1$ column vector representing the 2-D image $\alpha(x, y)$ that we wish to reconstruct,
- $\boldsymbol{\phi}$ is a $p \times 1$ vector of weights quantifying how much each element of $\boldsymbol{\alpha}$ contributes to the X-ray attenuation on the straight-line path ℓ,
- $\mu_0 < \mu_1 < \cdots < \mu_J$ are known discretization points along the μ axis, $\Delta\mu_j = \mu_j - \mu_{j-1}$, and
- $\mathcal{I}_j = \imath(\mu_j)\Delta\mu_j \approx \iota(\varepsilon_j)\Delta\varepsilon_j$.

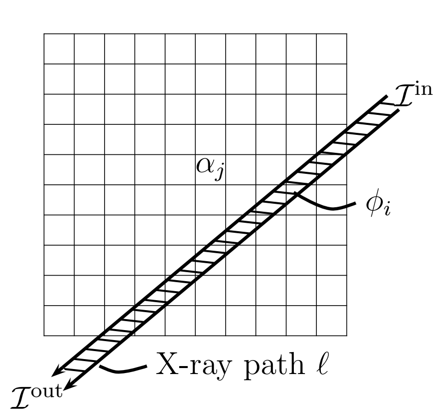

Figure 2: Discretization over space: $\int_\ell \alpha(x, y)\,\mathrm{d}\ell \approx \boldsymbol{\phi}^T\boldsymbol{\alpha}$.

The mass attenuation coefficient (MAC) discretization is facilitated by the following facts:
- μ of almost all materials at any energy level are within the range $10^{-2}\,\text{cm}^2/\text{g}$ to $10^4\,\text{cm}^2/\text{g}$,
- the energy level of an X-ray scan is usually selected so that the function $\mu(\varepsilon)$ is as flat as possible.

Choose discretization points $\{\mu_j\}_{j=1}^J$ with a sufficiently wide range to cover $\mu(\text{supp}(\iota(\varepsilon)))$:

$$\mu_j = \mu_0 q^j, \qquad j = 1, 2, \ldots, J. \tag{4}$$

Identifiability:
- The value of μ_0 in (4) can be arbitrary,
- if $\mathcal{I}_1 = 0$, $\mathcal{I}^{\text{out}}((\boldsymbol{\alpha}, [\mathcal{I}_1, \mathcal{I}_2, \ldots \mathcal{I}_J]^T)) \equiv \mathcal{I}^{\text{out}}((\boldsymbol{\alpha} q, [\mathcal{I}_2, \mathcal{I}_3, \ldots \mathcal{I}_J, 0]^T))$,
- if $\mathcal{I}_J = 0$, $\mathcal{I}^{\text{out}}((\boldsymbol{\alpha}, [\mathcal{I}_1, \mathcal{I}_2, \ldots \mathcal{I}_J]^T)) \equiv \mathcal{I}^{\text{out}}((\boldsymbol{\alpha}/q, [0, \mathcal{I}_1, \mathcal{I}_2, \ldots \mathcal{I}_{J-1}]^T))$.

Hence, if the range of $\{\mu_j\}_{j=1}^J$ is sufficiently large to allow for zero edge elements of $\boldsymbol{\mathcal{I}}$, then the recovery of $\boldsymbol{\alpha}$ will be correct up to a scale of common ratio q.

Measurement Model, Assumptions, and Constraints

An X-ray CT scan consists of multiple projections with the beam intensity measured by multiple detectors, see Fig. 3. Model a vector $\boldsymbol{z}$ of N log-scale noisy measurements as

$$\boldsymbol{z} = \boldsymbol{f}(\boldsymbol{\theta}) + \boldsymbol{n} = -\ln_\circ[A(\boldsymbol{\alpha})\boldsymbol{\mathcal{I}}] + \boldsymbol{n}$$

where $\ln_\circ(\boldsymbol{x})$ denotes elementwise logarithm,
- $\boldsymbol{\mathcal{I}} = [\mathcal{I}_1, \mathcal{I}_2, \ldots, \mathcal{I}_J]^T$,
- $\big[A(\boldsymbol{\alpha})\big]_{i,j} = \exp(-\Phi_{(i)}^T \boldsymbol{\alpha}\mu_j)$,
- $\Phi = [\Phi_{(1)}\Phi_{(2)} \cdots \Phi_{(N)}]^T$ is the Radon transform matrix for our imaging system, and
- $\boldsymbol{n}$ is additive white Gaussian noise.

Our goal: estimate the image and incident energy density parameters

$$\boldsymbol{\theta} = (\boldsymbol{\alpha}, \boldsymbol{\mathcal{I}}).$$

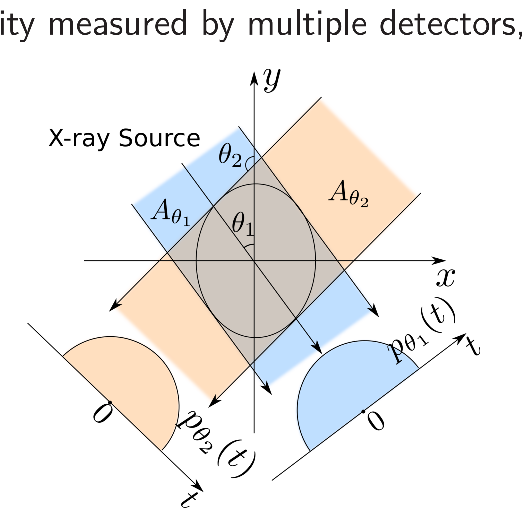

Figure 3: Projections at angles θ_1 and θ_2.

Assumptions:
- Object's shadow covered by the receiver array;
- Known upper bound $\mathcal{I}^{\text{in}}_{\text{MAX}}$ on incident energy $\mathcal{I}^{\text{in}}$: $\mathcal{I}^{\text{in}} = \sum_{j=1}^J \mathcal{I}_j = \mathbf{1}^T\boldsymbol{\mathcal{I}} \le \mathcal{I}^{\text{in}}_{\text{MAX}}$;
- $\imath(\mu)$ and $\alpha(x, y)$ are nonnegative for all ε, x and y: $\boldsymbol{\mathcal{I}} \succeq \mathbf{0}$ and $\boldsymbol{\alpha} \succeq \mathbf{0}$.

Notation: $\boldsymbol{y} \succeq \mathbf{0}$ denotes that all elements of a vector $\boldsymbol{y}$ are nonnegative.

Parameter Estimation

To leave some margin for the noise and discretization effects, we relax the nonnegative signal constraint $\boldsymbol{\alpha} \succeq \mathbf{0}$ and propose the following penalized least-squares (LS) objective function:

$$L_{\nu,t}(\boldsymbol{\theta}) = \frac{1}{2}\|\boldsymbol{z} - \boldsymbol{f}(\boldsymbol{\theta})\|_2^2 + \frac{\nu}{2}\underbrace{\|(-\boldsymbol{\alpha})_+\|_2^2}_{\text{energy of negative pixels}} + t\underbrace{\Big[-\mathbf{1}_{J\times1}^T \ln_\circ(\boldsymbol{\mathcal{I}}) - \ln\big(\mathcal{I}^{\text{in}}_{\text{MAX}} - \mathbf{1}_{J\times1}^T\boldsymbol{\mathcal{I}}\big)\Big]}_{\text{log barrier penalty}} \tag{5}$$

where ν and t are scalar tuning constants for the signal nonnegativity and sparsity penalty terms. Notation: $(\boldsymbol{x})_+$ keeps positive elements of $\boldsymbol{x}$ intact and sets the rest to zero.

Minimization Algorithm: Define the gradient vectors $\boldsymbol{g}_{\boldsymbol{\alpha},\nu}(\boldsymbol{\theta})$, $\boldsymbol{g}_{\boldsymbol{\mathcal{I}},t}(\boldsymbol{\theta})$ and Hessian matrices $H_{\boldsymbol{\alpha},\nu}(\boldsymbol{\theta})$, $H_{\boldsymbol{\mathcal{I}},t}(\boldsymbol{\theta})$ of the objective function (5) with respect to $\boldsymbol{\alpha}$ and $\boldsymbol{\mathcal{I}}$, respectively. Descend (5) by alternating between (i) and (ii):

(i) the Polak-Ribière *nonlinear conjugate-gradient step* for $\boldsymbol{\alpha}$ [Shewchuk 1994, Sec. 14.1] where $\boldsymbol{\mathcal{I}}$ is fixed and set to $\boldsymbol{\mathcal{I}}^{(i)}$;

$$\boldsymbol{\alpha}^{(i+1)} = \boldsymbol{\alpha}^{(i)} - s_{\boldsymbol{\alpha}} \frac{\boldsymbol{g}_{\boldsymbol{\alpha},\nu}^T(\boldsymbol{\theta}^{(i)})\boldsymbol{d}^{(i)}}{\boldsymbol{d}^{(i)T} H_{\boldsymbol{\alpha},\nu}(\boldsymbol{\theta}^{(i)})\boldsymbol{d}^{(i)}}\boldsymbol{d}^{(i)}$$

where

$$\boldsymbol{e}^{(i)} = \boldsymbol{g}_{\boldsymbol{\alpha},\nu}(\boldsymbol{\theta}^{(i)}) - \boldsymbol{g}_{\boldsymbol{\alpha},\nu}(\boldsymbol{\theta}^{(i-1)})$$

$$\beta^{(i)} = \max\Big\{0, \frac{\boldsymbol{g}_{\boldsymbol{\alpha},\nu}^T(\boldsymbol{\theta}^{(i)})\boldsymbol{e}^{(i)}}{\|\boldsymbol{g}_{\boldsymbol{\alpha},\nu}(\boldsymbol{\theta}^{(i-1)})\|_2^2}\Big\}$$

$$\boldsymbol{d}^{(i)} = \boldsymbol{g}_{\boldsymbol{\alpha},\nu}(\boldsymbol{\theta}^{(i)}) + \beta^{(i)}\boldsymbol{d}^{(i-1)};$$

(ii)
- if

$$\mathbf{1}_{N\times1} - \boldsymbol{z} + \boldsymbol{f}(\widetilde{\boldsymbol{\theta}}^{(i)}) \succeq \mathbf{0}_{N\times1} \tag{6}$$

holds, apply the *Newton step* for $\boldsymbol{\mathcal{I}}$:

$$\boldsymbol{\mathcal{I}}^{(i+1)} = \boldsymbol{\mathcal{I}}^{(i)} - s_{\boldsymbol{\mathcal{I}}}\Big[H_{\boldsymbol{\mathcal{I}},t}(\widetilde{\boldsymbol{\theta}}^{(i)})\Big]^{-1}\boldsymbol{g}_{\boldsymbol{\mathcal{I}},t}(\widetilde{\boldsymbol{\theta}}^{(i)})$$

where

$$\widetilde{\boldsymbol{\theta}}^{(i)} = (\boldsymbol{\alpha}^{(i+1)}, \boldsymbol{\mathcal{I}}^{(i)});$$

- otherwise, i.e., if (6) does not hold, keep the old $\boldsymbol{\mathcal{I}}$:

$$\boldsymbol{\mathcal{I}}^{(i+1)} = \boldsymbol{\mathcal{I}}^{(i)}.$$

Note: (6) ensures $H_{\boldsymbol{\mathcal{I}},t}(\widetilde{\boldsymbol{\theta}}^{(i)}) \ge 0$.

Numerical Example

Simulation example based on a binary 1024×1024 image in Fig. 5a obtained by thresholding the pixel values of a reconstruction in [Qiu and Dogandžić 2012, Fig. 5(b)].
- Inspected object, assumed to be made of iron, contains irregularly shaped inclusions; mass-attenuation function $\mu(\epsilon)$ for iron extracted from the NIST database.
- Polychromatic sinogram simulated using photon-energy discretization with 130 equi-spaced discretization points over the range 20 keV to 150 keV that approximates well the support of $\iota(\varepsilon)$.
- 1024-element measurement array employed.
- Radon transform Φ constructed using nonuniform fast Fourier transform (NUFFT) with full circular mask [Dogandžić et al. 2011].
- 180 equi-spaced parallel-beam projections with 1° spacing.
- Performance metric is the relative square error (RSE) of an estimate $\widehat{\boldsymbol{\alpha}}$ of the signal coefficient vector:

$$\text{RSE}\{\widehat{\boldsymbol{\alpha}}\} = 1 - \Big(\frac{\widehat{\boldsymbol{\alpha}}^T\boldsymbol{\alpha}}{\|\widehat{\boldsymbol{\alpha}}\|_2\|\boldsymbol{\alpha}\|_2}\Big)^2.$$

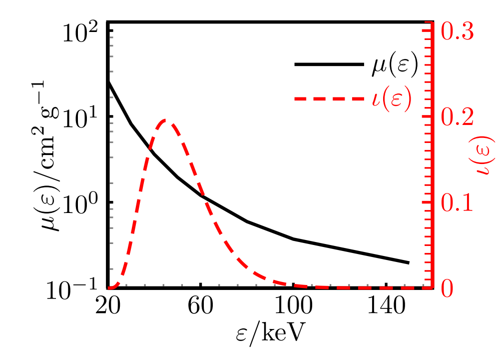

Figure 4: Simulated mass attenuation and incident X-ray spectrum as functions of the photon energy ε.

We compare
- the traditional filtered backprojection (FBP) method, and
- our MAC reconstruction upon convergence of the iteration (i)–(ii).

Figs. 5f and 5g show the histograms of the residuals $\boldsymbol{z} - \Phi\widehat{\boldsymbol{\alpha}}_{\text{FBP}}$ and $\boldsymbol{z} - \boldsymbol{f}(\boldsymbol{\theta}^{(+\infty)})$.

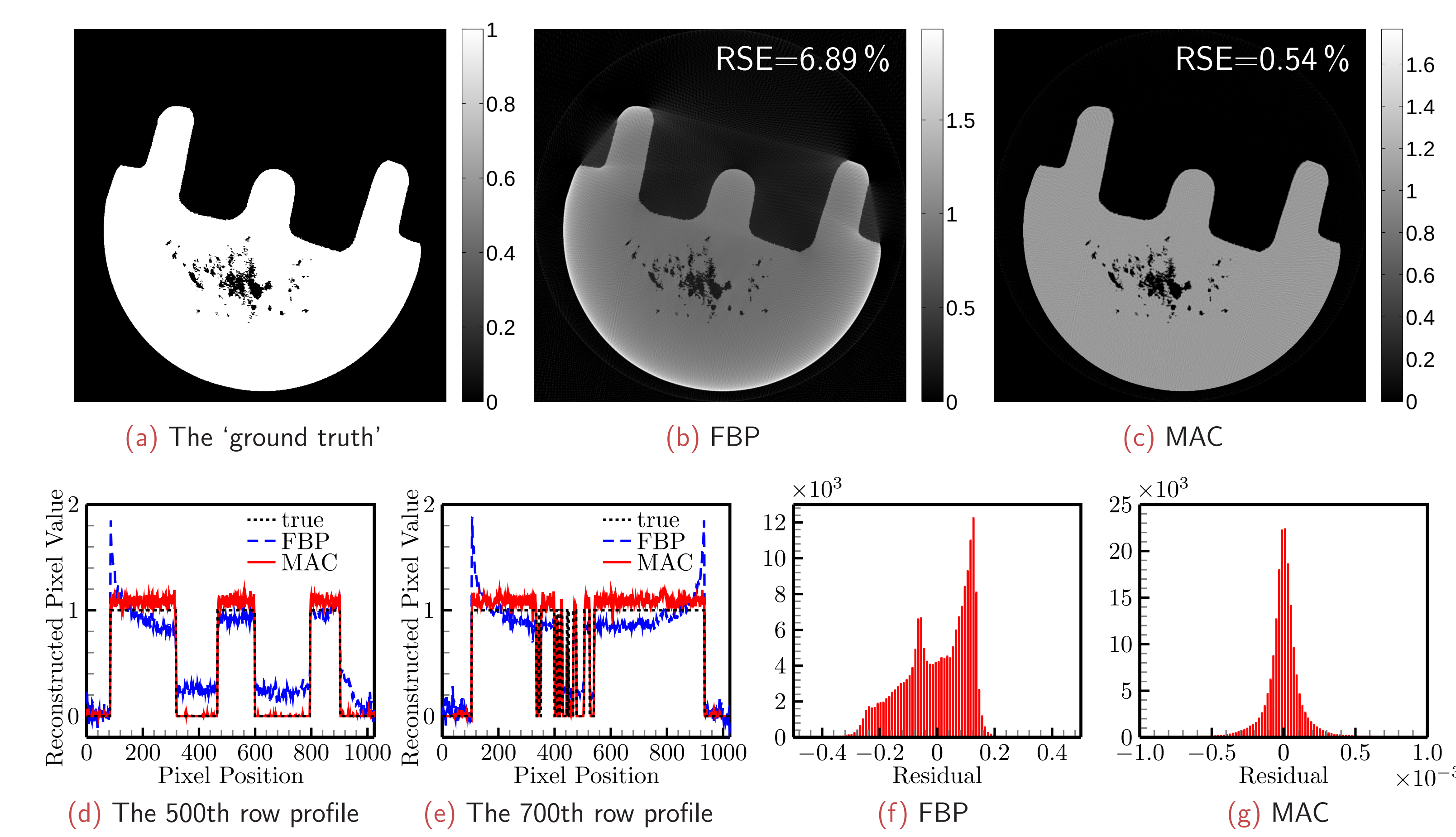

Figure 5: (a)–(c) The true image and FBP and MAC reconstructions, (d)–(e) corresponding 500th and 700th row profiles, and (f)–(g) residual histograms from the FBP and MAC reconstructions.

Future Work

- Generalize the proposed MAC discretization to handle multiple materials,
- Incorporate signal sparsity and develop an active set approach for estimating incident energy density parameters $\boldsymbol{\mathcal{I}}$ [Gu and Dogandžić 2013],
- Iteratively refine the selection of the mass attenuation discretization points $\{\mu_j\}_{j=1}^J$ based on the obtained estimates of $\boldsymbol{\mathcal{I}}$.

References

- Aleksandar Dogandžić, Renliang Gu, and Kun Qiu. "Mask iterative hard thresholding algorithms for sparse image reconstruction of objects with known contour." *Proc. Asilomar Conf. Signals, Syst. Comput.* Pacific Grove, CA, Nov. 2011, pp. 2111–2116.
- Renliang Gu and Aleksandar Dogandžić. *Sparse signal reconstruction from polychromatic X-ray CT measurements via mass attenuation coefficient discretization*. Tech. rep. NSF/IU. Ames, IA: CNDE, Iowa State Univ., Mar. 2013.
- Francis A Jenkins and Harvey E White. *Fundamentals of Optics*. 3rd ed. New York: McGraw-Hill, 1957.
- Kun Qiu and Aleksandar Dogandžić. "Sparse signal reconstruction via ECME hard thresholding." *IEEE Trans. Signal Process.* 60 (Sept. 2012), pp. 4551–4569.
- J. R. Shewchuk. *An introduction to the conjugate gradient method without the agonizing pain*. Tech. rep. CMU-CS-94-125. Pittsburgh, PA: Carnegie Mellon Univ., 1994.
- G. Van Gompel, K. Van Slambrouck, M. Defrise, K.J. Batenburg, J. de Mey, J. Sijbers, and J. Nuyts. "Iterative correction of beam hardening artifacts in CT." *Med. Phys.* 38 (2011), S36–S49.

Acknowledgment CENTER FOR NDE